Analysis of the Low-Frequency Isotropic Raman Spectrum of Molten Isotactic Polypropylene

V. M. Hallmark,† S. P. Bohan,‡ H. L. Strauss, and R. G. Snyder*

Department of Chemistry, University of California, Berkeley, California 94720

Received November 21, 1990

ABSTRACT: We have explored the feasibility of numerically calculating the low-frequency isotropic Raman spectrum of molten isotactic polypropylene to determine relations between the Raman spectrum and conformational disorder. The spectrum of the disordered polymer was approximated by summing the calculated spectra of a set of random conformers of 2,4,6,8,10,12,14,16,18-nonamethylnonadecane. The main features of the observed spectrum are reproduced in the calculated spectrum. Two spectra were calculated, one based on conformers generated from an isomeric three-state model and a second based on those from a five-state model. The two isomeric state models we employed have been previously described in the literature and used to calculate the colligative properties of molten polypropylene. The two spectra derived differ significantly mainly in the width of the "umbrella" band near 400 cm^{-1}. The observed width of this band can be accounted for only by the five-state model. In addition, the Raman spectrum of disordered isotactic polypropylene has been characterized. The distribution of intensity can be correlated with the frequency distribution of backbone and methyl modes. The D-LAM band, which is observed near 200 cm^{-1}, has two components rather than the one seen for molten polyethylene. We associate the two components with the two Raman-active zone-center modes of conformationally ordered $(gt)_\infty$ polypropylene.

I. Introduction

There are normally substantial differences between the vibrational spectra of a flexible polymer in its conformationally ordered and disordered states. This dependence of vibrational spectra on chain conformation can in principle be utilized to provide information about the conformational statistics of the disorder. The complexity of the spectra of assemblies of disordered chains makes this, however, extremely difficult to carry out effectively except in those special cases in which the chains are simple and short. Consequently, correlations between spectra and structure have remained largely empirical. A theoretical basis that relates the frequency and shape of a band in the spectrum of a highly disordered system to the conformational statistics of the constituent chains can sometimes be found.[1-3] The D-LAM band is an example. This band, which is formed by a superposition of bands from skeletal bending modes that are in some degree totally symmetric and thus exceptionally intense, appears prominently in the low-frequency isotropic Raman spectrum of the conformationally disordered polymethylene (PM) chain[1] and also in the isotropic Raman spectra of other disordered polymers.[2] In the case of the PM chain, the relation between the frequency of D-LAM and the concentration of gauche bonds has been quantitatively established.[1,3,4]

Direct calculation of the spectrum for comparison with the observed spectrum represents the broadest possible approach, since the entire spectrum or any region of it can be utilized for conformational analysis. Our recent numerical calculations on the vibrations and spectra of ensembles of simple disordered model chains indicate the possibilities.[3,5] Applications to assemblies of real chains in conformationally disordered state are as yet few in number and have been largely confined to short *n*-alkane chains.[6,7]

We report here on a numerical analysis of the low-frequency isotropic Raman spectrum of molten isotactic polypropylene (IPP). The aims of this study are to demonstrate that we can reproduce the observed spectrum and, as a result, characterize the spectrum and identify the factors that determine it. The calculated spectrum of the polymer is approximated by summing the calculated spectra of 1000 random conformers of 2,4,6,8,10,12,14,-16,18-nonamethylnonadecane (NMN).

II. Observed Spectra

The observed isotropic Raman spectrum of isotactic polypropylene in the molten state is shown in Figure 1 along with the spectra of two other vinyl polymers (isotactic poly(1-butene) and atactic polystyrene) and polyethylene, all in the molten state. The spectra were measured with a Spex Model 1403 spectrometer under a resolution of 4 cm^{-1}. The excitation was the 514.5-nm line of an argon ion laser. The isotropic spectra were obtained by subtracting $I_\perp$ from $I_\parallel$ to eliminate the anisotropic component from $I_\parallel$.

The spectra in Figure 1 all show a relatively intense band near 200 cm^{-1}. As noted above, this band, the D-LAM band, has been previously characterized in the case of the disordered polymethylene chain. The commonality of this band for each polymer suggests that the modes contributing to it are similar in character, even though the chains themselves have different side groups. The peak frequency and width of the D-LAM bands are also similar, and this suggests that the proportion of trans and gauche bonds in the skeleton is likewise similar.[1-3]

The spectra of the vinyl polymers differ in some ways from the spectrum of PE. The 200-cm^{-1} band in the vinyl spectra tends to be more complex, sometimes appearing as a doublet. The principal difference, however, is in the high-frequency band near 400 cm^{-1}. Our earlier normal coordinate analysis of crystalline IPP indicates that this band represents the "umbrella" mode, in which the CCC angles centered around the tertiary carbon open and close in phase.[8] The 400-cm^{-1} band occurs, therefore, in the spectra of all the vinyl polymers.

The spectrum of polystyrene shown in Figure 1 is that of the atactic polymer, and this raises questions concerning

† Present address: IBM Almaden Research Center, San Jose, CA 95120-6099.

‡ Present address: Analytical Research Department, Rohm and Haas, Bristol, PA 19007.

0024-9297/91/2224-4025$02.50/0

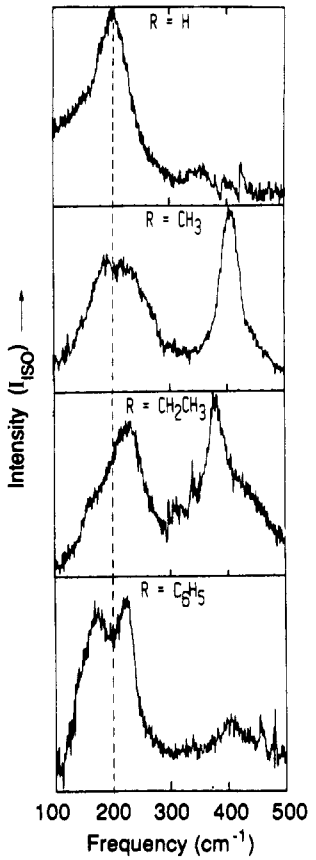

Figure 1. Low-frequency isotropic Raman spectra of molten polyethylene (R = H) at 480 K, isotactic polypropylene (R = CH_3) at 490 K, isotactic poly(1-butene) (R = CH_2CH_3) at 520 K, and atactic polystyrene (R = C_6H_5) at 480 K.

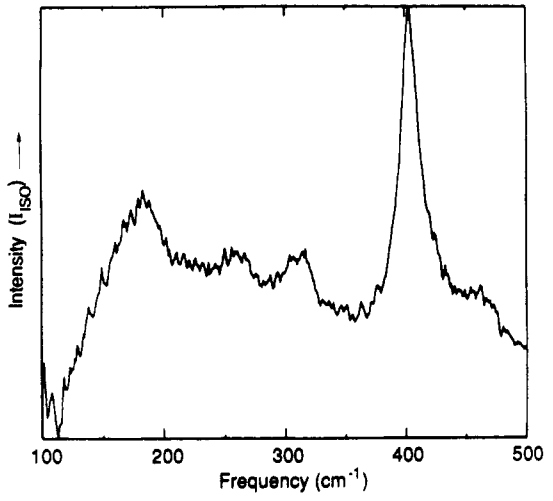

Figure 2. Low-frequency isotropic Raman spectrum of atactic polypropylene at 300 K.

the effect of tacticity on the spectra of disordered vinyl polymers. We will not pursue the subject other than to mention that, not unexpectedly, differences in tacticity, like differences in conformational disorder, are indeed reflected in the spectra. The spectrum of molten atactic polypropylene near 300 K is shown in Figure 2 and is found to be significantly different from that of the isotactic form shown in Figure 1.

Figure 3 shows Raman spectra of polycrystalline IPP at 300 K and of molten IPP near 500 K. The spectrum of the latter is shown both in terms of the parallel and perpendicular components and in terms of the isotropic component.

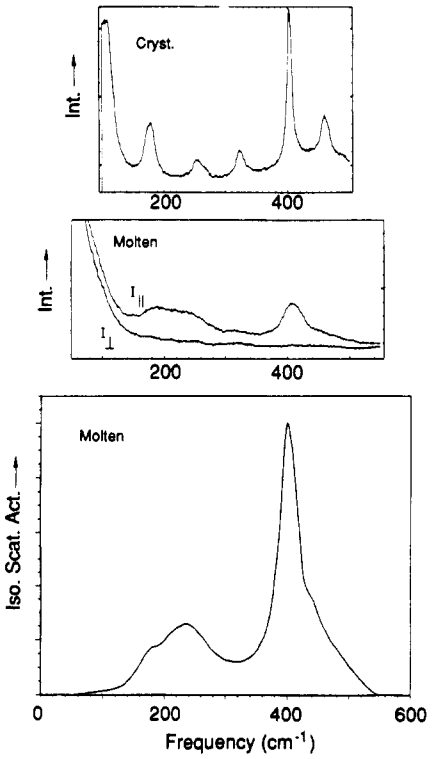

Figure 3. Raman spectra of isotactic polypropylene: crystalline powder (295 K); parallel ($I_\parallel$) and perpendicular $I_\perp$ components of the spectrum of the liquid (500 K); isotropic spectrum of the liquid (500 K) with intensity expressed in terms of scattering activity.

III. Calculation of Spectra

A. Spectrum of a Single Conformer of NMN. To reduce the time required to compute the low-frequency spectrum, we reduced the size of the NMN conformers by eliminating the hydrogens. The mass of each carbon was increased by the masses of these hydrogens. The effect of eliminating the hydrogens is to reduce the number of modes per conformer to 78, of which approximately 2/3 are the skeletal-deformation modes that contribute intensity in the low-frequency region of the isotropic spectrum. The parameters used to define the structure of each conformer are characterized as follows. All CCC bond angles were assumed to be tetrahedral, and all CCC bond lengths were assigned a value of 1.54 Å. The values of the dihedral angles define the conformation of the NMN chains. How the conformers were generated will be discussed in the next section.

To obtain accurate vibrational frequencies under the skeletal approximation, it is necessary to determine a force field appropriate to the simplified structure. The use of a subset of force constants selected from a set defined and evaluated for the complete hydrocarbon chain leads to calculated frequencies that are seriously in error. For example, if a subset from a valence force field (VFF) derived for saturated unstrained hydrocarbons[9] is used for the IPP skeleton, the calculated frequency of the tertiary carbon umbrella band is about 100 cm^{-1} higher than the observed frequency. Most other features in the calculated spectrum undergo frequency displacements of a similar magnitude. The reason that the subset performs so poorly has to do mainly with the redundancy associated with the angle-deformation internal coordinates about the tetrabonded carbon. The force constants associated with the six bending coordinates centered about a tetrahedral carbon are interdependent. Therefore, if the HCH and HCC bending coordinates are eliminated, the value of the

Table I
Skeletal Valence Force Field for Isotactic Polypropylene

descrip	constant[a]	skeletal value[b]	approx std error[c]	with hydrogens (ref 9) value[b]
stretch CC				
	K_R	4.337[d]		4.337
	K_S	4.387[d]		4.387
bend CCC				
	H_A	1.113	0.024	1.130
	H_B	1.481	0.128	
	H_C	1.082	0.025	1.084
	H_D	0.993	0.017	
torsion CCC				
	H_τ	0.015[d]		0.024
stretch/stretch				
	F_{RR}, F_{RS}	0.101[d]		0.101
stretch bend				
	F_{SB}	−0.544	0.115	
	F_{SC}	0.113	0.051	
	F_{RC}	1.018	0.039	0.417
	F_{RA}	0.568	0.027	
	F_{RB}	0.362	0.041	
bend/bend				
	F_{BC}	0.124	0.016	
	F_{CC}	0.201	0.016	−0.041
	F_{CD}	0[e]		
	f^a	0[e]		−0.011
	f^s	0[e]		0.011

[a] The internal coordinates are defined in Figure 4. [b] The units for stretch are mdyn Å^{-1} and for bend and torsion mdyn Å rad^{-2}. Those for the interaction constants are appropriately compatible. [c] Estimated from the standard error in the frequency parameters and variance–covariance matrix. [d] Not adjusted. [e] Cound not be determined.

CCC bending force constant must be reevaluated.[10]

It was necessary therefore to evaluate a valence force field for the IPP chain skeleton. A description of this VFF is summarized in Table I. The internal coordinates used are defined in Figure 4. The "reference" frequencies used to evaluate the force constants are those of 15 conformers that were selected as being representative of a set of 100 randomly generated conformers of 2,4,6,8,-10,12-hexamethyltridecane (HMT). These reference frequencies are the frequencies calculated for the 15 conformers with their hydrogens in place. The force field used to obtain the reference frequencies is given in ref 9. The errors in the frequencies thus obtained are estimated to be ±8 cm^{-1}.

Only those reference frequencies below 600 cm^{-1} were used in evaluating the simplified force field, since a skeletal force field does not, of course, reproduce the frequencies of modes above 600 cm^{-1} with much accuracy because these modes for the complete molecule involve significant hydrogen motion.

The distribution of frequency errors is displayed in Figure 5. The differences are between frequencies calculated with the skeletal VFF and the reference frequencies obtained from the full calculation. The number of force constants adjusted was 11, and the number of reference frequencies was 493. The average error is 3.3 cm^{-1} overall and around 6 cm^{-1} in the region 600–100 cm^{-1}. We note from Table I that many of the force constants, especially the interaction force constants, have values that are

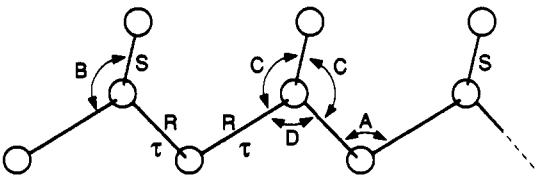

Figure 4. Definitions of the internal coordinates used in the calculation of vibrational frequencies. R and S are CC stretches; A, B, C, and D are CCC angle deformations; τ is CCCC torsion.

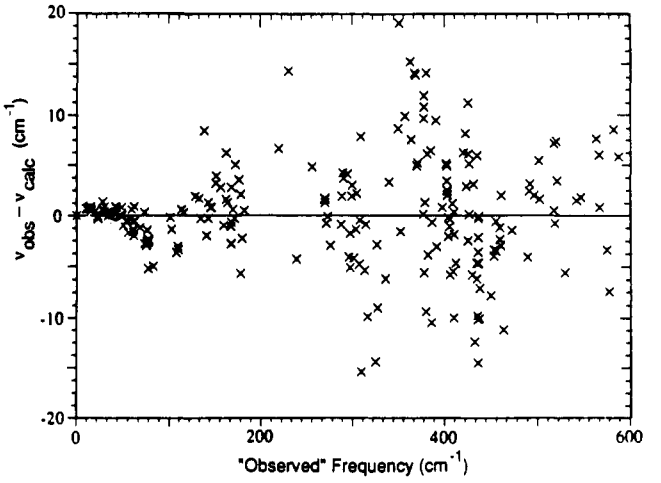

Figure 5. Frequency distribution of the differences between the calculated and the "reference" frequencies of the vibrational modes used in the evaluation of the skeletal force constants listed in Table I. (See text for meaning of "reference".)

significantly different from those of the saturated hydrocarbon force field. This is not surprising since the physical significance of the values of the skeletal force constants has been obscured.

A measure of the suitability of the skeletal approximation is how well the low-frequency dispersion curves for the $(gt)_\infty$ chain are reproduced. Figure 6 shows these curves calculated in the skeletal approximation and also for the chain with the hydrogens included. The curves are very similar for the two calculations. The full calculation results in a branch near 200 cm^{-1} that does not appear if the hydrogens are not present. This branch is associated with methyl torsion, which is essentially inactive in the Raman.

The isotropic Raman intensity of each mode was estimated on the basis of a bond polarizability model. Our earlier analysis of cyclohexane indicated that, although C–C stretching is the primary contributor to the isotropic Raman intensity, there is a significant contribution from CCC bending.[5,11] More recent analyses of cyclohexane[12] and propane[13] have confirmed both the applicability of the bond moment model and the necessity to include both C–C stretching and CCC bending terms. The scattering activity, S_k, of the kth normal mode may be expressed

$$S_k = [\sum_i^{CC} \bar{\alpha}'_{CC} L_{ik} + \sum_j^{CCC} \bar{\alpha}'_{CCC} L_{jk}]^2 \qquad (1)$$

where $\bar{\alpha}'_{CC}$ and $\bar{\alpha}'_{CCC}$ are the derivatives of the mean parameters for C–C stretching and CCC bending with respect to the kth normal coordinate and where L_{ik} and L_{jk} are the eigenvalue elements for stretching and bending, respectively. In our calculation, the values used for the ratio $\bar{\alpha}_{CCC}/\bar{\alpha}_{CC}$ were between 0.2 and 0.3. These values are in the range reported in the literature which is summarized in ref 6.

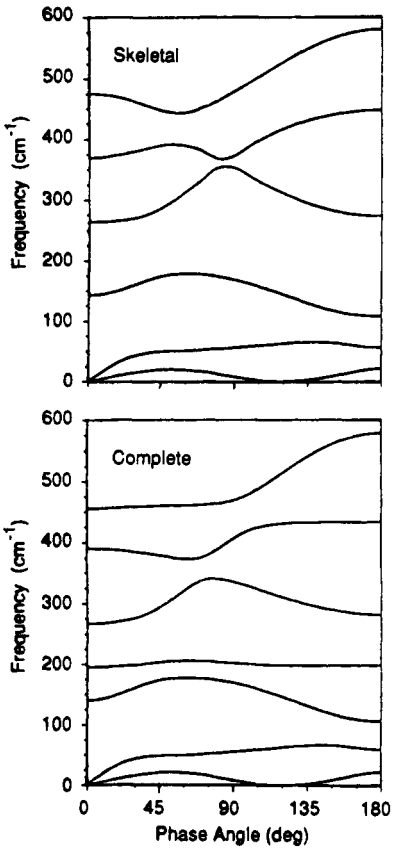

Figure 6. Dispersion curves calculated for the $(gt)_\infty$ IPP chain: top, skeletal approximation; bottom, complete chain.

The scattering activity, S_k, and Raman intensity, I_k, are related through the expression

$$I_k \propto [\nu_k(1 - \exp(h\nu_k/kT)]^{-1}S_k \qquad (2)$$

where ν_k is the frequency of mode k and where T is the temperature of the sample.[11] The intensities in the observed and calculated spectra are expressed in terms of scattering activity.

B. Conformer Generation for the Three- and Five-State Models. Conformationally random chains of IPP were generated with the use of conditional probabilities, q_{ij}, which are the probabilities that a bond will be in conformational state j, given that the preceding bond is in state i. The values of the q_{ij} can be derived from the statistical weights associated with the set of conformational states chosen to represent the potential energy surface. The methods have been described by Flory.[14] The conformational statistics of the set of 1000 random conformers that we generated was checked by evaluating directly the (second order) a priori probabilities, p_{ij}, and then comparing the values with the values of the p_{ij} derived from the statistical weights.[14]

Relative to the PM chain, the potential energy surface of IPP is significantly more complex due to the spatial asymmetry introduced by the methyl side groups. The greater complexity of IPP requires the inclusion of *two* skeletal CC bonds, rather than one, for the purpose of generating conformers and describing the conformational statistics of the assembly.

Two models of a potential energy surface for describing short-range interactions in IPP have been invoked by Flory and his co-workers in their efforts to calculate the conformational statistics and colligative properties of this polymer. The simpler model is the "three-state" model[15] in which the conformational states of the skeletal backbone are essentially those of the PM chain; that is, there are three staggered conformations that correspond to t, g, and g′ states.[14] The similarity between PM and IPP at the three-state level does not, of course, extend to the actual values of the statistical weights, which are quite different for the two polymers.

The second model, known as the "five-state" model, may be considered an extension of the three-state model, in which two more isomeric states are introduced.[16] These latter states are associated with CC bond conformations that tend to be nearly eclipsed and consequently are of higher energy. In our calculations we have used the statistical weights for five-state models that were derived from the potential energy surface described in ref 16. The values of the dihedral angles associated with local minima in the three-state and five-state models are listed in Table II.

Table II
Dihedral Angles Used for the Three- and Five-State Models of Polypropylene

model	desig of state[a]	dihedral angle (τ)
three-state	t	180
	g	60
	g′	−60
five-state[b]	t	165
	t*	130
	g	75
	g′	−65
	g*	110

[a] The asterisks denote the nearly eclipsed conformations. [b] The dihedral angles are from ref 16.

Table III
Computed Values of the First- and Second-Order Probabilities for the Three- and Five-State Models of Isotactic Polypropylene at 500 K[a]

Three-State

t	0.538	tt	0.206
g	0.233	tg + tg′	0.664
g′	0.229	gg + g′g′	0.054
		gg′	0.076

Five-State

t	0.430	tt	0.062	g*g	0.025
t*	0.160	tt*	0.174	g*g′	0.016
g	0.327	t*t*	0.009	gg′	0.024
g*	0.038				
g′	0.045	tg*	0.026	g*g*	0.000
		tg	0.524	gg	0.000
		tg′	0.014	g′g′	0.000
		t*g*	0.010		
		t*g	0.082		
		t*g′	0.037		

[a] The parameters used to calculate the probabilities are as follows. For the three-state model: E_τ = 500 cal/mol and E_ω = 2000 cal/mol. For the five-state model:[16] $\eta = 1.0 \exp(-60/RT)$; $\tau = 0.4 \exp(-500/RT)$; $\omega^* = 0.9(-1600/RT)$.

The conformational statistics of IPP and PM based on the two models are compared in Tables III and IV. In Table III the first- and second-order probabilities for the three- and five-state models are summarized for IPP at 500 K, the approximate temperature at which the Raman measurements were made. In Table IV the statistics calculated for IPP are compared with those of PM at the same temperature.

The first-order probabilities are similar for PE and IPP, provided we classify all states into t or g categories. This may be seen in Table IV, where we note that the similarity is greatest between PM and five-state IPP. The second-order probabilities for IPP reflect the characteristic propensity of the IPP chain to assume conformations in

Table IV
Comparison of the Computed Probabilities for Polyethylene (PM) and Isotactic Polypropylene (IPP)

	PM (500 K)[a]	IPP (500 K)[b]	
		3-state	5-state[c]
t	0.578	0.538	0.590
g + g′	0.422	0.462	0.410
tt	0.298	0.206	0.244
tg + tg′	0.560	0.664	0.691
gg + g′g′	0.131	0.054	0.000
gg′	0.021	0.076	0.065

[a] The parameters used for PM are 0.5 kcal/mol for the g energy and 2.0 kcal/mol for the gg′ energy, both relative to the trans state. [b] The parameters used to calculate the probabilities are listed in Table II. [c] The distinction between the two trans states has been removed and likewise for the various gauche states. (Compare Table III.)

which t and g (or t and g′) bonds alternate in order to minimize the overlap of methyl groups on adjacent monomer units. The chains in crystalline IPP have a $(tg)_\infty$ conformation,[17] but for the molten state at 500 K only about 2/3 of the adjacent bond pairs are predicted to have a tg conformation for either the three- or five-state model. The fraction of tg pairs for molten IPP is calculated to be significantly greater than that for PM.

IV. Discussion

As already noted, the isotropic Raman spectrum of IPP has been approximated as the sum of the spectra of 1000 random conformers of NMN. Self-overlapping NMN chains were excluded. The calculated isotropic spectra and densities of vibrational states are displayed in the figures as histograms with 4-cm^{-1} intervals.

A. Comparison with Observed Spectrum: Three-State versus Five-State Model. The observed isotropic Raman spectrum of molten IPP at 500 K is shown in Figure 7, along with spectra that we calculated on the basis of the three-state and the five-state models. The values of the parameters used in the calculation are indicated. In general, there is good agreement between the calculated and observed spectra. The calculated spectra show the main features of the observed spectrum: a broad band near 220 cm^{-1} that consists of two overlapping components; a narrower band near 400 cm^{-1} that has a broad shoulder on the high-frequency side.

An important question is which of the two calculated spectra—that based on the three-state model or that based on the five-state model—agrees better with the observed spectrum.

A preference for the spectrum derived from the five-state model is found on the basis of the width of the 400-cm^{-1} band. The half-width (fwhh) observed for this band is about 35 cm^{-1}. The half-width obtained from the calculated spectrum is about 12 cm^{-1} for the three-state model and about 25 cm^{-1} for the five-state model. The greater breadth found for the five-state model probably arises from the additional inhomogeneous broadening from the two high-energy conformational states. We note that the "natural" width (fwhh) of isotropic Raman bands in this frequency region for a sample near room temperature is probably between 7 and 10 cm^{-1}: Tanabe and Jonas, for example, report of about 9 cm^{-1} for the 386-cm^{-1} band of liquid cyclohexene,[18] and we have measured values around 8 cm^{-1} for the liquid *n*-alkanes for bands that are not appreciably affected by fluctuations of the CC bond rotational angles.[6]

A possibility that must be considered is that the width of the 400-cm^{-1} band in the calculated spectrum might be determined by CC torsional fluctuations in the skeletal backbone of the IPP chain. In that case, the above argument favoring the five-state model would not hold. We note that torsional broadening has indeed been observed to be a significant source of Raman band broadening for the liquid *n*-alkanes.[6,9]

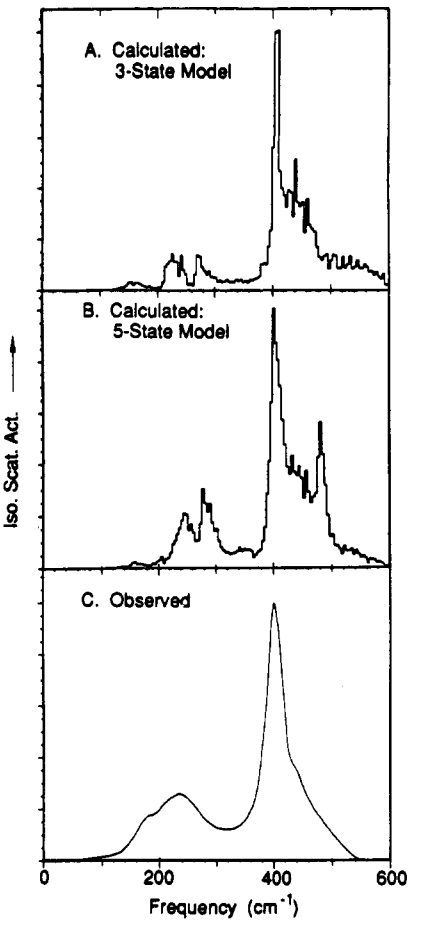

Figure 7. Isotropic Raman spectra of disordered isotactic polypropylene as represented by NMN: (A) calculated spectrum based on the three-state model (E_τ = 500 cal/mol, E_ω = 2000 cal/mol, R = 0.2, T = 500 K); (B) calculated spectrum based on the five-state model (η, τ, and ω^* are given in Table III, R = 0.2, T = 500 K); (C) observed spectrum of IPP at 500 K.

The magnitude of the effect of torsional fluctuations on the spectrum of IPP can be estimated. Fluctuations were simulated by allowing the values of the CC torsional angles of the skeleton to assume a Gaussian distribution centered about the equilibrium value. Calculated spectra based on three-state model ensembles are shown in Figure 8 for standard deviations in the torsional angles ranging from 0 to 50°. Over this range, the width of the 400-cm^{-1} band is found to be nearly unaffected. A similar result would be expected for the five-state model. We conclude then that torsional angle fluctuations do not significantly contribute to the breadth of the 400-cm^{-1} band, and therefore the above argument favoring the five-state model remains valid.

Additional spectroscopic evidence favoring the five-state model comes from the fact that the calculated spectrum based on the five-state model is overall in somewhat better agreement with the observed spectrum than that from the three-state model. In particular, the ratios of the intensity of the 400-cm^{-1} band to the intensities of the bands in the 250- and 550–500-cm^{-1} regions are in better accord with the observed ratio. On the other hand, the five-state spectrum shows a band near 490 cm^{-1}, corresponding to the shoulder observed near 490 cm^{-1}. The sharpness of

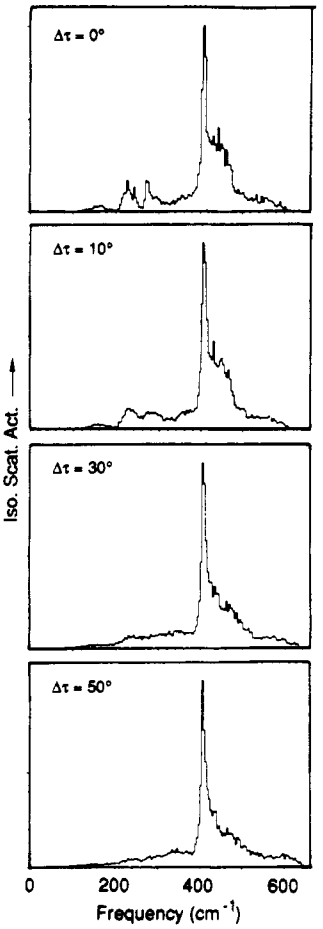

Figure 8. Isotropic Raman spectrum of isotactic polypropylene (NMN) at 500 K calculated for the three-state model under the condition that the CCCC dihedral angles of the skeletal backbone have a Gaussian distribution about the equilibrium values. The standard deviations, $\Delta\tau$, are indicated. (E_τ = 500 cal/mol, E_ω = 2000 cal/mol, R = 0.3.)

the feature at 490 cm^{-1} may be an artifact due to inadequate conformational statistics.

Finally, we note that the effect of randomness in the dihedral angles is noticeable in the calculated spectra in promoting broadening and smoothing of most features, yielding a spectrum that in overall appearance more nearly resembles the observed spectrum. Although torsional fluctuations must occur, little is known about their magnitude. An estimate of the degree of static fluctuation for amorphous glassy atactic polypropylene at −40 °C has been made by Theodorou and Suter[20] from atomistic modeling. Their results indicate a standard deviation around 16° for both t and g bonds.

B. Assignments. The low-frequency Raman spectrum of IPP would seem to divide naturally at 300 cm^{-1} into two regions. The region above 300 cm^{-1} contains the 400-cm^{-1} band and, underlying this band and extending to higher frequencies, a broad, partially obscured background. The 400-cm^{-1} band is known to be associated with the $C(C)_3$ umbrella bending mode that is centered on the tertiary carbon atom. The region below 300 cm^{-1} consists of the D-LAM related band near 220 cm^{-1}. As noted earlier, this band is a doublet (Figure 1).

The origin and distribution of Raman intensity are indicated from calculated spectra in which the intensity contribution from the skeletal backbone or the tertiary carbon $C(C)_3$ group is suppressed. Such spectra are shown in Figure 9. In the case in which the intensity originates from the $C(C)_3$ groups, it appears almost entirely in the

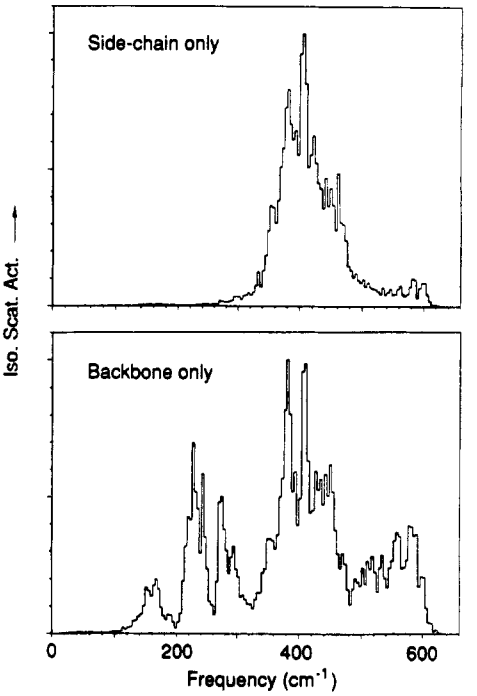

Figure 9. Calculated isotropic Raman spectrum of IPP (NMN): top, skeletal-backbone intensity contributions suppressed; bottom, side-chain intensity suppressed. (Three-state model, T = 500 K, T_τ = 500 cal/mol, E_ω = 2000 cal/mol.)

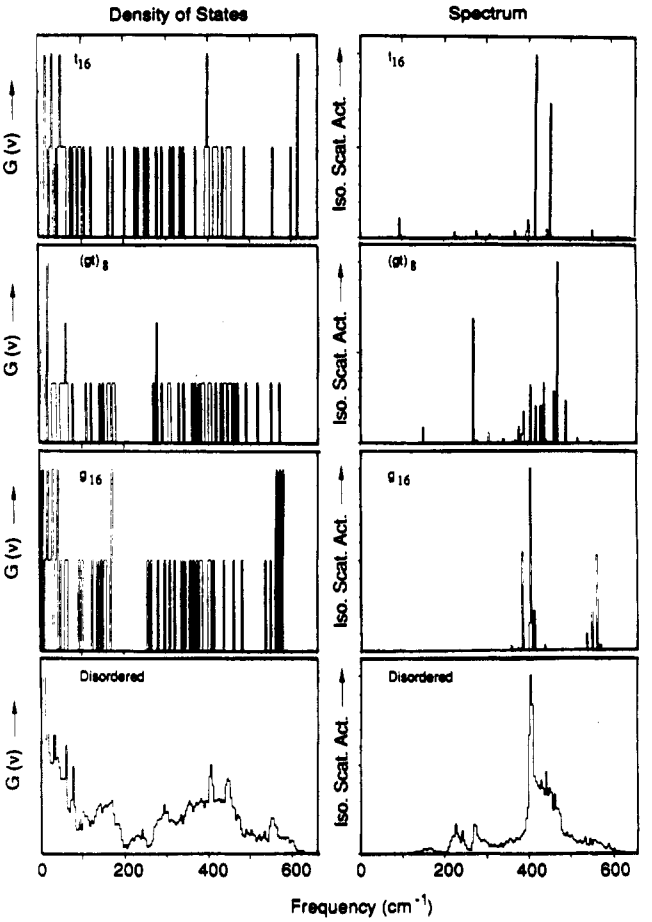

Figure 10. Density of states and isotropic Raman spectra of NMN chains in the ordered conformations t_{16}, $(gt)_8$, and g_{16} and in an assembly of disordered conformations. (Parameters used in the disordered-chain calculation are those given in the caption for Figure 7 for the three-state model.)

400-cm^{-1} band. In the case in which the intensity originates from the skeletal backbone, it is broadly distributed in

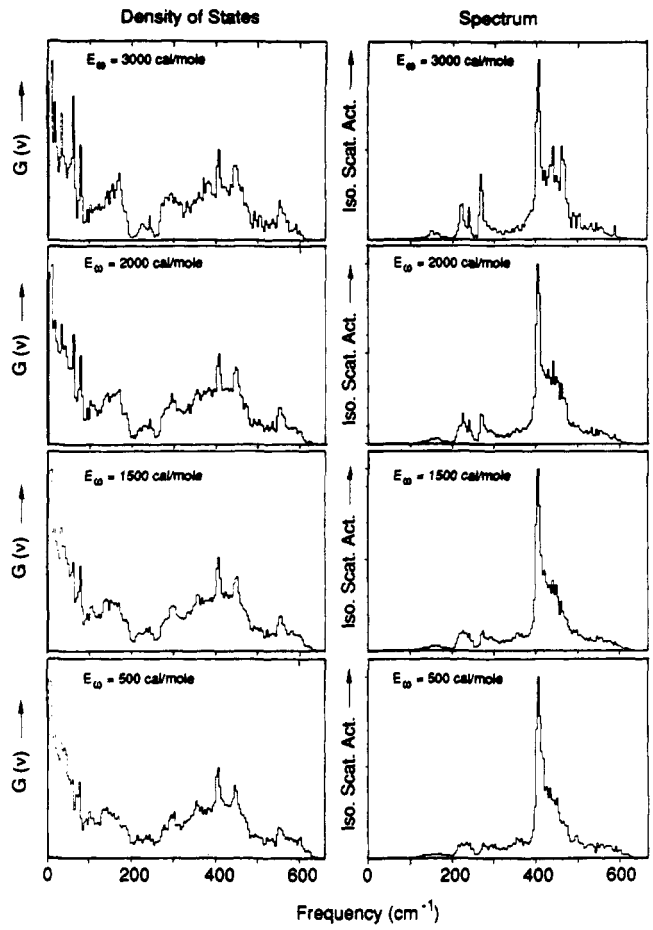

Figure 11. Density of states and isotropic Raman spectra of IPP (NMN) at 500 K calculated for the three-state model with the values of E_ω indicated. (E_τ = 500 cal/mol, R = 0.3.)

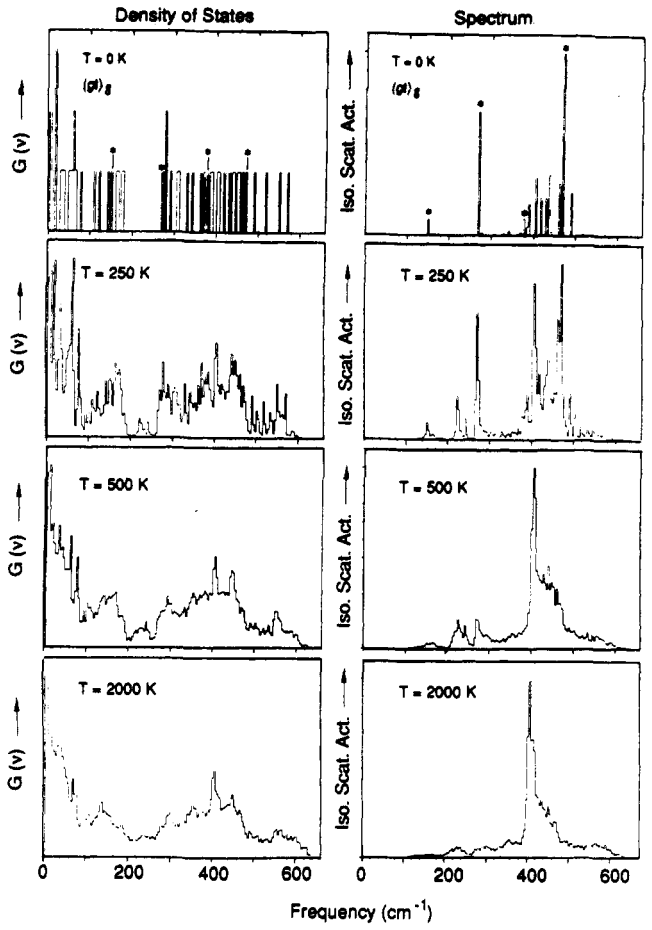

Figure 12. Density of states and isotropic Raman spectra of IPP (NMN) calculated for the three-state model at the indicated temperatures. The asterisks in the density of states and spectrum for T = 0 K indicate the frequencies at the zone center. (E_τ = 500 cal/mol, E_ω = 2000 cal/mol, R = 0.3.)

the spectrum, making up the two D-LAM bands (220 and 280 cm^{-1}) and extending into the $C(C)_3$ region. The intensity distribution is broad because the backbone modes interact with the modes of the $C(C)_3$ groups.

We note that the distribution of vibrational modes and Raman intensity in the spectrum of disordered IPP bears a resemblance to that for conformationally ordered chains. This may be seen in Figure 10, which shows the calculated density of states and spectra of the t_{16}, $(gt)_8$, and g_{16} conformers of NMN and of disordered IPP as represented by NMN. In addition, we note that for the ordered chains the frequency center of the density of states and intensity tends to move to a higher value as the concentration of gauche bonds increases. Similar trends have also been found for the polymethylene chain.[6]

The complexity of the calculated spectra of conformationally ordered IPP chains, such as is found for the $(gt)_8$ conformer in Figure 10, is much greater than that expected solely from a consideration of zone-center selection rules and, if found in an observed spectrum, might well be interpreted to indicate conformational disorder. On the basis of selection rules alone, the spectrum of the $(gt)_8$ chain should show only four prominent bands in the frequency region considered. These bands correspond to the four zone-center modes that are Raman active for the infinite $(gt)_\infty$ chain. The additional bands appear due to the finite length of the chain, the low symmetry of the repeat unit, and the fact that the dispersion curves associated with the $(gt)_\infty$ chain have maxima and minima (Figure 6). These conditions allow extensive intramolecular interactions between modes whose frequencies are close together, with the result that intensity gets distributed among many of the interacting modes. This is discussed in some detail in ref 6 for the *n*-alkanes, although the phenomenon is less pronounced for the *n*-alkanes than for IPP.

Finally, we consider the question of why *two* D-LAM bands appear in the Raman spectrum of molten IPP. As noted earlier, these bands have maxima near 235 and 180 cm^{-1} and appear with comparable intensity in the observed spectrum, although, if the spectrum is expressed in terms of scattering activity (Figure 3), the 235-cm^{-1} component is significantly more intense. We associate these bands with the two isotropic, Raman-active zone-center modes that are found near 265 and 140 cm^{-1} for the ordered $(gt)_\infty$ chain (Figure 6). Our calculations indicate that for $(gt)_\infty$ the intensity of the higher frequency band at 265 cm^{-1} is greater. From these considerations we can account, at least qualitatively, for the frequencies and relative intensities of both component bands. The association of D-LAM bands with zone-center modes is valid, provided the conformation of the ordered chain represents to a good approximation of the average conformation of the disordered chains. Thus, for the polymethylene chain, the frequency of the D-LAM band of molten polyethylene is near 200 cm^{-1},[1] while the calculated frequency of the zone-center mode of the acoustical branch for the $(gt)_\infty$ chain is 216 cm^{-1}.[21]

C. Dependence on E_ω and T. The effect of the "pentane" interaction energy, E_ω, on the calculated density of states and isotropic Raman spectra of IPP at 500 K is indicated in Figure 11. The values chosen for E_ω range

between 500 and 3000 cal/mol, thus including values that are well below and above the accepted ones. The effect of changing E_ω over this range of values is not very great. The most apparent effect is a tendency for spikelike features to appear at low frequencies for the largest values of E_ω. These features reflect a reduction in disorder. The density of states and isotropic spectra are more sensitive to the "butane" interaction energy, E_τ, since vibrations are more sensitive to short-range interactions. (The dependence of spectra on E_τ is not considered here.)

Some measure of the temperature dependence of both the density of states and the isotropic spectrum of the IPP chain is indicated in Figure 12. The ordered $(gt)_n$ chain, which we have already considered, is associated with the temperature 0 K. (The asterisks in Figure 12 in the density of states and spectrum at $T = 0$ K indicate the zone-center frequencies.) At 250 K, the main features associated with an assembly of highly disordered chains are present. For example, the spectrum at 250 K shows bands near 220 cm^{-1} that are components of the D-LAM band.

It is noteworthy that, as the temperature increases, the high-frequency cutoff for the density of states and for Raman intensity, which is near 600 cm^{-1} at 250 K, moves to significantly higher frequencies. Since the cutoff frequency is well-defined in the measured spectrum, it can be used as a measure of disorder.

Acknowledgment. We gratefully acknowledge the support of this research through grants from the National Science Foundation (DMR 87-01586) and the National Institutes of Health (GM 27690). In addition, we thank Dr. Yesook Kim for measuring the Raman spectrum of atactic polypropylene and Professor Leo Mandelkern of Florida State University for supplying us with that sample.

References and Notes

(1) Snyder, R. G. *J. Chem. Phys.* **1982**, *76*, 3921–3927.
(2) Snyder, R. G.; Wunder, S. W. *Macromolecules* **1986**, *19*, 496–498.
(3) Snyder, R. G.; Strauss, H. L. *J. Chem. Phys.* **1987**, *87*, 3779–3788.
(4) Mandelkern, L.; Alamo, R.; Mattice, W. L.; Snyder, R. G. *Macromolecules* **1986**, *19*, 2404–2408.
(5) Snyder, R. G. *Macromolecules* **1990**, *23*, 2081–2087.
(6) Snyder, R. G.; Kim, Yesook *J. Phys. Chem.* **1991**, *95*, 602–610.
(7) Machida, K.; Noma, H.; Miwa, Y. *Indian J. Pure Appl. Phys.* **1988**, *26*, 197.
(8) Snyder, R. G.; Schachtschneider, J. H. *Spectrochim. Acta* **1964**, *20*, 853–869.
(9) Snyder, R. G.; Schachtschneider, J. H. *Spectrochim. Acta* **1965**, *21*, 169–195.
(10) Wilson, E. B.; Decius, J. C.; Cross, P. C. *Molecular Vibrations*; McGraw-Hill: New York, 1955.
(11) Snyder, R. G. *J. Mol. Spectrosc.* **1970**, *36*, 204–221.
(12) Gough, K. M.; Murphy, W. F. *J. Chem. Phys.* **1988**, *87*, 1509–1519.
(13) Gough, K. M.; Murphy, W. F.; Stroyer-Hansen, T.; Svendsen, E. Norby *J. Chem. Phys.* **1988**, *87*, 3341–3346.
(14) Flory, P. J. *Statistical Mechanics of Chain Molecules*; Wiley-Interscience: New York, 1969.
(15) Flory, P. J.; Mark, J. E.; Abe, A. *J. Am. Chem. Soc.* **1966**, *88*, 631.
(16) Suter, U. W.; Flory, P. J. *Macromolecules* **1975**, *8*, 765–776.
(17) Natta, G.; Corradini, P.; Ceseari, M. *Atti Accad. Naz. Lincei, Rend. Cl. Sci. Fis. Mat. Nat.* **1956**, *21*, 365.
(18) Tanabe, K.; Jonas, J. *Chem. Phys.* **1979**, *38*, 131.
(19) MacPhail, R. A.; Snyder, R. G. *J. Chem. Phys.* **1989**, *91*, 3895.
(20) Theodorou, D. N.; Suter, U. W. *Macromolecules* **1985**, *18*, 1467.
(21) Snyder, R. G. *J. Chem. Phys.* **1967**, *47*, 1316.